

# The Interpretation and Implication of the Afterglow of GRB 060218

Yizhong Fan<sup>1,2,3\*</sup>, Tsvi Piran<sup>1</sup> † and Dong Xu<sup>4</sup>

<sup>1</sup>*The Racah Inst. of Physics, Hebrew University, Jerusalem 91904, Israel*

<sup>2</sup>*Purple Mountain Observatory, Chinese Academy of Science, Nanjing 210008, China*

<sup>3</sup>*National Astronomical Observatories, Chinese Academy of Sciences, Beijing 100012, China*

<sup>4</sup>*Dark Cosmology Centre, Niels Bohr Institute, University of Copenhagen, Juliane Maries Vej 30, 2100 Copenhagen, Denmark*

Accepted ..... Received .....; in original form .....

## ABSTRACT

The nearby GRB 060216/SN 2006aj was an extremely long, weak and very soft GRB. While it was peculiar in many aspects its late ( $> 10^4$  sec) X-ray afterglow showed a canonical power law decay. Assuming that this component arises due to a relativistic blast wave decelerated by a circumburst matter we infer that the blast wave's kinetic energy was rather high,  $5 \times 10^{50}$  erg, close to what is seen in other GRBs. The lack of a “jet break” implies that the outflow was wide  $\theta_j \sim 1$ . The rather weak early optical emission rules out a dense circumburst wind profile. It also constrains the initial Lorentz factor to be significantly lower than usual,  $\Gamma_{\text{ini}} \sim 15$ . The observed afterglow suggests that the medium surrounding a massive star progenitor (up to distances of  $\sim 10^{17} - 10^{18}$  cm) is not the expected dense stellar wind (a similar result was seen in many other bursts and in particular in GRB 030329). This implies that the progenitor's wind was weak during the last 100-1000 years before the burst. This interpretation requires a different source for the thermal emission seen in the early X-ray and late optical/UV. We speculate that this emission arises from the interaction of the relativistic ejecta with the stellar envelope.

**Key words:** Gamma Rays: bursts–ISM: jets and outflows–radiation mechanisms: nonthermal–X-rays: general

## 1 INTRODUCTION

GRB 060218 (Cusumano et al. 2006a) was a nearby ( $z=0.033$ , Mirabal & Halpern 2006; Cusumano et al. 2006b) burst associated with a bright type Ic broad-lines SN (Modjaz et al. 2006; Sollerman et al. 2006; Pian et al. 2006). It is distinguished in several aspects from other bursts: (i) It is very long ( $T_{90} \sim 2000$  sec). (ii) The prompt  $\gamma$ -ray and X-ray luminosity is extremely low  $\sim 10^{47}$  erg s<sup>-1</sup> (Sakamoto et al. 2006) and the overall isotropic equivalent  $\gamma$ -ray energy, a few  $\times 10^{49}$  erg, is small compared to typical bursts. (iii) The prompt emission is very soft and it contains a soft thermal component in the X-ray band. The thermal emission begins at  $\sim 152$  sec and continues up to  $\sim 10^4$  sec. (iv) A second thermal component in the UV/optical band peaks at  $t \sim 10^5$  sec after the GRB trigger (Campana et al. 2006). (v) For  $t > 10^4$  sec, the XRT lightcurve is simple and is well described a single power-law decay  $t^{-1.15}$  with no

break (Campana et al. 2006). While the prompt emission is very different from a typical GRB and the optical emission is complicated by the appearance of the thermal bump and the supernova signal this last component, the X-ray afterglow, is rather typical.

We focus here on this X-ray afterglow, which can be interpreted in terms of the standard afterglow model, and use it as a key to understand what has happened in this burst. One can infer from it the kinetic energy,  $E_k \sim 5 \times 10^{50}$  erg, as well as the wide opening angle,  $\theta_j \sim 1$ , of the relativistic component of the ejecta. One can also infer, from a combined analysis of this and the optical afterglow that the initial Lorentz factor was rather small as compared to typical GRBs.

The association with a type Ic SN suggests that the progenitor was a WR-star (Campana et al. 2006). One expects, therefore, that the central engine is surrounded by a dense stellar wind, like the one seen in GRB 980425 that was associated with SN 98bw (Li & Chevalier 1999; Waxman 2004). However, the density nearest to the progenitor depends on the mass loss rate during the latest phases of the

\* Lady Davis Fellow, E-mail: yzfan@pmo.ac.cn

† tsvi@phys.huji.ac.il

WR-star, which is unknown at present (Woosley, Zhang & Heger 2003). Using the X-ray and optical data we show that the circumburst medium surrounding the progenitor has a constant low density. Since the ejecta is very wide this conclusion cannot be attributed to anisotropy in the mass loss as has been suggested for GRB 030329<sup>1</sup>.

The low luminosity of the prompt emission as well as the soft spectrum might be attributed to a viewing angle. This possibility has been questioned by Nousek et al. (2006). We show (in sec. 3) that while such a model is compatible with the X-ray and optical afterglow light curves (for a constant density circumburst matter profile) it requires a very large prompt energy as well as a very large ratio of prompt energy to kinetic energy. Furthermore, the small ratio of the offset viewing angle to the jet opening angle makes this interpretation unlikely.

We examine possible sources for the thermal emission in section 4. Our conclusions and the implications for the GRB/SN connection are discussed in section 5.

## 2 THE MULTI-WAVELENGTH AFTERGLOW

The late ( $> 10^4$  sec) X-ray afterglow is similar to the one seen in typical GRBs in its overall intensity as well as in the almost standard power law decay index. In the standard GRB afterglow model (Sari, Piran & Narayan 1998; Piran 1999), the X-ray afterglow is produced by a blast wave that is slowed down by a constant density circumburst medium. The bulk Lorentz factor is:

$$\Gamma \approx 3.4 E_{k,51}^{1/8} n_0^{-1/8} t_d^{-3/8} (1+z)^{3/8}, \quad (1)$$

where  $n$  is the number density of the surrounding matter, and  $t_d$  is the observer's time in days. The lack of a "jet-break" (Rhoads, 1999; Sari et al, 1999; Halpern et al., 1999) in the X-ray afterglow lightcurve in the range  $t \sim 0.1 - 10$  days suggests a very wide opening angle:

$$\theta_j > 1/\Gamma(t_d = 10) = 0.7 E_{k,51}^{-1/8} n_0^{1/8} t_{d,1}^{3/8} (1+z)^{-3/8}. \quad (2)$$

The emission of the shock is determined by the peak flux,  $F_{\nu,\max}$  and by the synchrotron and cooling frequencies,  $\nu_m$  and  $\nu_c$  (Sari, Piran & Narayan 1998; Yost et al. 2003):

$$F_{\nu,\max} = 63.9 \text{ mJy} (1+z) D_{L,26.7}^{-2} \epsilon_{B,-2}^{1/2} E_{k,51} n_0^{1/2}, \quad (3)$$

$$\nu_m = 5.4 \times 10^{10} \text{ Hz} E_{k,51}^{1/2} \epsilon_{B,-2}^{1/2} \epsilon_{e,-1}^2 C_p^2 (1+z)^{1/2} t_d^{-3/2}, \quad (4)$$

$$\nu_c = 2 \times 10^{16} \text{ Hz} E_{k,51}^{-\frac{1}{2}} \epsilon_{B,-2}^{-\frac{3}{2}} n_0^{-1} (1+z)^{-\frac{1}{2}} t_d^{-\frac{1}{2}} \frac{1}{(1+Y)^2}, \quad (5)$$

where  $D_L$  is the corresponding luminosity distance,  $p$  is the power-law index of the shocked electrons, we use  $p = 2.3$  throughout this work, and  $C_p \equiv 13(p-2)/[3(p-1)]$ .  $Y = (-1 + \sqrt{1 + 4\eta\eta_{KN}\epsilon_e/\epsilon_B})/2$  is the Compton parameter, where  $\eta = \min\{1, (\nu_m/\nu_c)^{(p-2)/2}\}$  (Sari, Narayan &

<sup>1</sup> The optical afterglow of GRB 030329 can be fitted reasonably well with a constant density model (e.g., Berger et al. 2003; Huang, Cheng & Gao 2006). However, the ejecta of GRB 030329 is very narrow ( $\sim 0.05$  rad) and the ISM-like medium may be caused by an anisotropic mass loss of the progenitor (Woosley et al. 2003).

Piran 1996; Wei & Lu 1998),  $0 \leq \eta_{KN} \leq 1$  is a coefficient accounting for the Klein-Nishina effect (Fan & Piran 2006).

The flux recorded at  $t_d = 0.1$  by XRT,  $\mathcal{F} = 2 \times 10^{-11} \text{ ergs s}^{-1} \text{ cm}^{-2}$ , should be compared with the theoretical prediction (assuming the XRT energy range  $\nu_X > \max\{\nu_c, \nu_m\}$ ):

$$\begin{aligned} \mathcal{F} &= \int_{\nu_{X1}}^{\nu_{X2}} F_{\nu_X} d\nu_X \\ &= 1.4 \times 10^{-10} \text{ ergs s}^{-1} \text{ cm}^{-2} (1+z)^{(p+2)/4} D_{L,26.7}^{-2} \\ &\quad \epsilon_{B,-2}^{(p-2)/4} \epsilon_{e,-1}^{p-1} E_{k,51}^{(p+2)/4} (1+Y)^{-1} t_{d,-1}^{(2-3p)/4}, \end{aligned} \quad (6)$$

where  $\nu_{X1} = 0.2$  keV and  $\nu_{X2} = 10$  keV. The agreement suggests that the typical parameters used here are consistent with the observation.

While the X-ray afterglow after  $10^4$  sec seem regular the optical and ultraviolet afterglows are very peculiar. The early data ( $t_d \leq 0.02$ ) seems to be the low energy tail of the prompt X-ray/γ-ray non-thermal emission. On the other hand the late long-wavelength afterglow ( $0.4 < t_d < 1.4$ ) is also dominated by a thermal component (Campana et al. 2006). With the extinction correction (Guenther et al. 2006), the spectral index of the UBV emission, at this time, is about 2 for  $\nu < 10^{15}$  Hz.

If  $\Gamma_{\text{ini}} > 35$ , the V-band afterglow should peak at  $t_d \sim 0.002$  (see eq.[1]) with a flux  $\sim 64$  mJy  $\epsilon_{B,-2}^{1/2} E_{k,51} n_0^{1/2}$ . This is much stronger than the observed flux (see Fig.1). A possible resolution of this contradiction is that the initial Lorentz factor is small  $\Gamma_{\text{ini}} \sim 15$ . In this case the UV/optical afterglow peaks at  $t_d \sim 0.06$ . The V-band flux should be

$$\begin{aligned} F_{\nu_V}^{\text{w}} &\approx 0.1 \text{ mJy} (1+z)^{\frac{p+3}{4}} D_{L,26.7}^{-2} E_{k,51}^{\frac{p+3}{4}} n_0^{1/2} \epsilon_{e,-1}^{p-1} C_p^{p-1} \\ &\quad \epsilon_{B,-2}^{\frac{p+1}{4}} t_d^{\frac{-3(p-1)}{4}}. \end{aligned} \quad (7)$$

Note that a factor 1/64 has been taken into account when evaluating  $F_{\nu,\max}$  since the radius of the shock front satisfies  $R \approx 2\Gamma^2 ct$  rather than  $R \approx 8\Gamma^2 ct$  for  $t_d < 0.06$ . This flux is compatible with the observations.

Fig. 1 depicts a comparison of the theoretical the multi-wavelength afterglow lightcurves with the observations. Here the synchrotron-self-absorption effect has been taken into account but the external Inverse Compton cooling of the shocked electrons, caused by the long term prompt X-ray/γ-ray emission, has not. Such a simplification is mainly for the reduction of the calculation. Therefore, both the X-ray and the optical emission at  $t < 0.1$  day have been overestimated. The actual fluxes should be lower, which are consistent with the observations. The initial Lorentz factor ( $\Gamma_{\text{ini}} \sim 15$ ) used to avoid a strong early optical emission is significantly lower than typical Lorentz factors inferred in GRBs.  $\Gamma_{\text{ini}}$  cannot be much smaller than this value. The X-ray flux declines as a single power-law at  $t \sim 9 \times 10^3$  sec, implies that the blast wave obtained the Blandford-McKee profile at this stage. This poses a lower limit on the initial Lorentz factor of the outflow of  $\Gamma > 8 E_{k,51}^{1/8} n_0^{-1/8} t_{d,-1}^{-3/8}$ .

In the stellar wind model (Dai & Lu 1998; Mészáros, Rees & Wijers 1998),  $n = 3 \times 10^{35} A_* R^{-2} \text{ cm}^{-3}$ , where  $A_* = [\dot{M}/10^{-5} M_{\odot} \text{ yr}^{-1}] [v_w/(10^8 \text{ cm s}^{-1})]$  (Chevalier & Li 2000),  $\dot{M}$  is the mass loss rate of the progenitor,  $v_w$  is the velocity of the wind. The bulk Lorentz factor of the outflow can

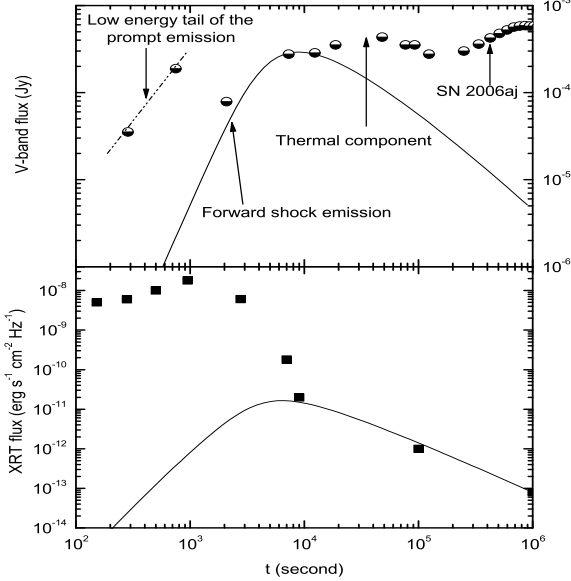


**Figure 1.** A comparison of the observed (Campana et al. (2006)) XRT and V-band afterglow lightcurves of GRB 060218 with the (numerical) predictions for the forward shock emission in the constant density circumburst medium (solid line). The parameters used are:  $E_k = 5 \times 10^{50}$  erg,  $\Gamma_{\text{ini}} = 15$ ,  $\theta_j = 1$ ,  $\epsilon_e = 0.1$ ,  $\epsilon_B = 0.01$ ,  $n = 0.5 \text{ cm}^{-3}$  and  $p = 2.3$ .

be estimated by (the superscript “w” represents the wind model):

$$\Gamma^w \approx 2E_{k,51}^{1/4} A_*^{-1/4} t_d^{-1/4} (1+z)^{1/4}. \quad (8)$$

Following Chevalier & Li (2000) the equations that govern the forward shock emission are:

$$F_{\nu, \text{max}}^w = 1.4 \text{ Jy} (1+z)^{3/2} \epsilon_{B,-2}^{1/2} E_{k,51}^{1/2} A_* t_d^{-1/2} D_{L,26.7}^{-2}, \quad (9)$$

$$\nu_m^w \approx 4 \times 10^{10} \text{ Hz} \epsilon_{e,-1}^2 C_p^2 E_{k,51}^{1/2} \epsilon_{B,-2}^{1/2} (1+z)^{1/2} t_d^{-3/2}, \quad (10)$$

$$\nu_c^w \approx 10^{14} \text{ Hz} \epsilon_{B,-2}^{-3/2} E_{k,51}^{1/2} A_*^{-2} (1+z)^{-3/2} t_d^{1/2} (1+Y)^{-2}. \quad (11)$$

We estimate the expected XRT energy flux as:

$$\mathcal{F}^w \approx 1.8 \times 10^{-10} \text{ erg s}^{-1} \text{ cm}^{-2} \epsilon_{B,-2}^{\frac{p-2}{4}} E_{k,51}^{\frac{p+2}{4}} t_{d,-1}^{\frac{-(3p-2)}{4}} D_{L,26.7}^{-2} \epsilon_{e,-1}^{p-1} C_p^{\frac{p+2}{4}} (1+z)^{\frac{p+2}{4}} (1+Y)^{-1}. \quad (12)$$

The canonical value is a few times that of the XRT observation of GRB 060218  $\sim 2 \times 10^{-11} \text{ erg s}^{-1} \text{ cm}^{-2}$  at  $t_d \sim 0.1$  (note that  $Y \sim$  a few). On the other hand, assuming  $\nu_V > \max\{\nu_c^w, \nu_m^w\}$ , the V-band flux is:

$$F_{\nu_V}^w \approx 22 \text{ mJy} \epsilon_{B,-2}^{\frac{p-2}{4}} E_{k,51}^{\frac{p+2}{4}} t_{d,-1}^{\frac{-(3p-2)}{4}} D_{L,26.7}^{-2} \epsilon_{e,-1}^{p-1} C_p^{\frac{p+2}{4}} (1+z)^{\frac{p+2}{4}} (1+Y)^{-1}. \quad (13)$$

If we normalize  $\mathcal{F}^w$  as  $\sim 2 \times 10^{-11} \text{ erg s}^{-1} \text{ cm}^{-2}$  then  $F_{\nu_V}^w \sim 3 \text{ mJy}$ , which is brighter by a factor of 10 than the observed flux  $\sim 0.3 \text{ mJy}$ . In other words, a contrast between V-band flux and the X-ray flux smaller than  $\mathcal{R} \equiv F_{\nu_V}^w / F_{\nu_X}^w \approx (\nu_X / \nu_V)^{p/2}$  is needed. This could be, for example,  $\nu_X > \nu_c^w > \nu_V$  and  $\nu_c^w \sim 100\nu_V \sim 5 \times 10^{16} \text{ Hz}$  at  $t_d \sim 0.1$ , requiring a very small  $A_*$  ( $\sim 0.01$ ) and/or very small  $\epsilon_B$  ( $\sim 10^{-5}$ ). In this case, we have  $F_{\nu_V}^w / F_{\nu_X}^w = (\nu_X / \nu_V)^{1/2} (\nu_X / \nu_V)^{(p-1)/2} \sim 0.1\mathcal{R}$ , which is

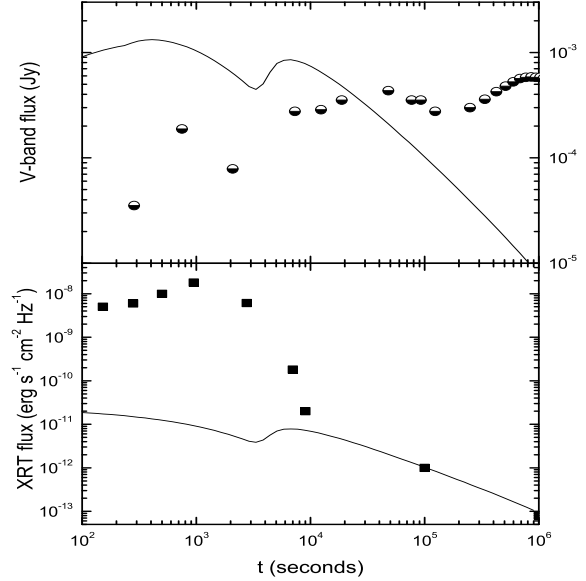


**Figure 2.** A comparison of the observed (Campana et al. (2006)) XRT and V-band afterglow lightcurves of GRB 060218 with the (numerical) predictions for the forward shock emission in the wind case (solid line). The parameters used are:  $E_k = 10^{51}$  erg,  $\Gamma_{\text{ini}} = 4$ ,  $\theta_j = 1$ ,  $\epsilon_e = 0.2$ ,  $\epsilon_B = 0.01$ ,  $A_* = 1$  and  $p = 2.3$ . The troughs are caused by the external inverse Compton cooling. As shown in the upper panel, the wind model is incompatible due to its too bright optical emission.

compatible with the data. However, this is unlikely because  $\nu_c^w \sim 5 \times 10^{16} \text{ Hz} t_{d,-1}^{1/2}$ , which is in the XRT energy range for  $t_d > 1$ . The X-ray temporal and spectral indices ( $\alpha_X$  and  $\beta_X$ ) thus change to be  $-(1-3p)/4$  and  $-(p-1)/2$  rather than  $-(2-3p)/4$  and  $-p/2$  (Chevalier & Li 2000). Both the temporal steepening and the spectral flattening were not seen in GRB 060218. The other possible scenario is  $\nu_c^w > \nu_X > \nu_V$ , which also yields  $F_{\nu_V}^w / F_{\nu_X}^w = (\nu_X / \nu_V)^{(p-1)/2} \sim 0.1\mathcal{R}$ . But in this case, the spectral and temporal indices should be  $-(p-1)/2$  and  $-(1-3p)/4$  respectively. As  $\alpha_X \sim -1.2$  this implies  $p \sim 2$  and  $\beta_X \sim -0.5$ , which is inconsistent with the observed  $\beta_X \sim -2.3 \pm 0.6$  at  $t_d \sim 3$  (De Luca 2006). We therefore conclude that a dense wind model is unlikely.

For illustration, we compare in Fig. 2 the (numerically calculated) predicted V-band and X-ray afterglow lightcurves with the observations. Both synchrotron-self absorption and early external inverse Compton cooling, caused by the prompt  $\gamma$ -ray/X-ray emission, have been taken into account. To calculate the external inverse Compton cooling, we have approximated the external photon luminosity as  $L_{ph} \sim 1.5 \times 10^{46} \text{ erg s}^{-1}$  for  $t < 3000 \text{ s}$  and  $L_{ph} \sim 1.5 \times 10^{46} \text{ erg s}^{-1} (t/3000)^{-5.2}$  for  $3000 \text{ s} < t < 9000 \text{ s}$ , otherwise  $L_{ph} \sim 0$ . The external inverse Compton parameter is calculated as  $Y_{EIC} \approx U_{ph}/U_B$ , where  $U_{ph} = L_{ph}/(4\pi R^2 \Gamma^2 c)$ ,  $U_B = 1.8 \times 10^{33} \text{ erg cm}^{-3} \epsilon_B \Gamma^2 R^{-2}$  is the magnetic energy density at the shock front. The troughs in Fig. 2 are caused by the external inverse Compton cooling. As expected from our analytical argument we could not find proper parameters that fit the data. The calculated early V-band flux is too bright to match the observation.

An alternative scenario suggested by Waxman (2004) for GRB 980425 is that the source of the X-ray afterglow is

a sub-relativistic outflow. However, in this case the kinetic energy of the ejecta satisfies  $E_k \sim 10^{48} \text{ erg } \beta^3 A_*(t_{\text{dec}}/0.1\text{d})$ , where  $\beta$  is the velocity of the ejecta, in units of  $c$ ,  $t_{\text{dec}}$  is the deceleration timescale of the ejecta. For such small  $E_k$  ( $\sim 10^{48} \text{ erg}$ ), it is straightforward to show that the resulting X-ray flux at  $t_{\text{dec}} \sim 0.1$  day is 2 to 3 order lower than the data.  $A_* \gg 1$  permits a much larger  $E_k$  and could give rise to X-ray emission as strong as the detected one. But the resulting UV/optical emission at  $t_{\text{dec}}$  is, once more, too bright to be consistent with the data.

We summarize this section by reiterating our conclusions. The X-ray afterglow from  $10^4$  sec to  $10^6$  sec is well fitted by a wide angle relativistic blast wave propagating into a constant density circumburst medium. The kinetic energy of the blast wave is  $E_k = 5 \times 10^{50} \text{ erg}$ . Considering the wide opening angle the total energy of this relativistic ejecta is comparable to the one seen in typical GRB afterglows (Panaitescu & Kumar, 2001; Frail et al. 2001; Piran et al. 2001). On the other hand the combination of the X-ray lightcurve and the earlier low optical/UV emission limits the initial Lorentz factor as  $8 < \Gamma_{\text{ini}} < 15$ . With this interpretation both the early ( $< 10^4$  sec) thermal X-ray emission and the late ( $\sim 4 \times 10^4 - 10^5$  sec) optical thermal emission must arise from a different component and not from the relativistic blast wave.

### 3 THE CONS AND PROS OF AN OFF-AXIS JET

A highly beamed emission observed off axis would result be seen as soft and weak, like in this burst. Nousek et al. (2006) argue against the possibility that GRB 060218 was a regular GRB viewed off axis. In this case the peak of the forward shock emission should be monochromatic, whereas in GRB 060218 the X-ray emission peaks at  $t \leq 10^4$  sec and the UV/optical emission peaks at  $t \sim 4 \times 10^4$  sec. This argument becomes irrelevant if we interpret the UVOT thermal component as arising from a different source. In this scenario, the forward shock UV/optical emission peaked at  $t \sim 10^4$  sec but the late UV/optical afterglow lightcurve is dominated by the thermal component produced by the hot expanding envelope. In this case the outflow could be an off-axis jet. Fig. 3 depicts a numerical calculation of the afterglow for an off-axis jet. The expected lightcurve is consistent with the data.

For an off-axis jet propagating into a constant density circumburst medium the detection timescale satisfies<sup>2</sup>:

$$dt_{\text{off}} \approx [1 + (\Gamma \Delta \theta)^2] dt, \quad (14)$$

<sup>2</sup> Previously, it is widely believed that the duration of an off-axis GRB should be much longer than it viewed on-axis. This viewpoint may be invalid when the GRB is powered by the internal shocks. Surely, the duration of one pulse should be extended by a factor of  $\sim 1 + (\Gamma_{\text{ini}} \Delta \theta)^2$ , but the total duration is still dominated by the activity timescale of the central engine (which would be unchanged for different viewing angle) unless the duration of one pulse is comparable with that of the burst. Therefore, statistically speaking, in the internal shock GRB model, the duration of the off-beam events may be just slightly longer than that of the on-beam bursts.

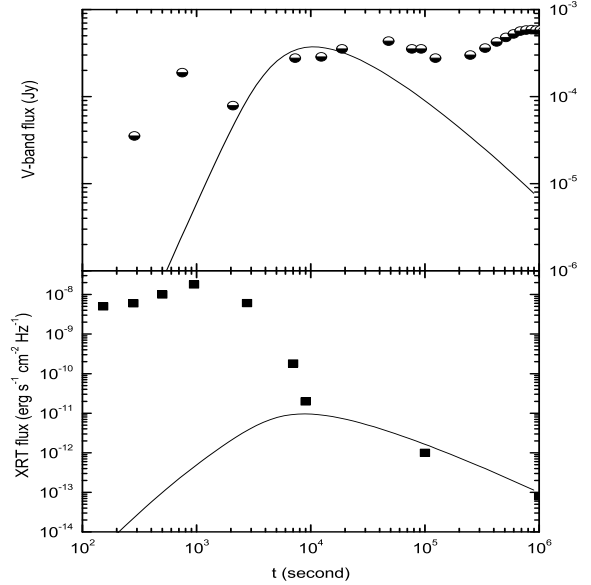


**Figure 3.** A comparison of the observed XRT and V-band afterglow lightcurve of GRB 060218 with the expected forward shock lightcurve of a blast wave powered by an off-axis ejecta expanding into the medium with a constant density (solid line). The parameters used are:  $E_k = 10^{51} \text{ erg}$ ,  $\Gamma_{\text{ini}} = 30$ ,  $\theta_j = 0.6$ ,  $\Delta\theta = 0.05$ ,  $\epsilon_e = 0.15$ ,  $\epsilon_B = 0.01$ ,  $z = 0.033$ ,  $n = 1 \text{ cm}^{-3}$  and  $p = 2.3$ .

where  $\Delta\theta$  is the angle between the line of the sight and the edge of the jet and the subscript “off” represents the off-axis case. When the flux begins to drop normally,  $\Gamma \sim 1/\Delta\theta$ ,  $t_{\text{off}} \sim 2t$  and thus

$$\Delta\theta \approx 0.1 E_{k,51}^{-1/8} n_0^{1/8} t_{\text{off},-1}^{3/8} (1+z)^{-3/8}. \quad (15)$$

The detected prompt X-ray and  $\gamma$ -ray energy satisfies

$$E_{\gamma,\text{obs}} \approx \frac{E_{\gamma,0}}{[1 + (\Gamma_{\text{ini}} \Delta\theta)^2]^3}, \quad (16)$$

where both energies are the isotropic equivalent energies. Now  $E_{\gamma,\text{obs}} \sim 10^{50} \text{ erg}$  yields  $E_{\gamma,0} \sim 10^{53} \text{ erg}$ . Given the fact that the jet is very wide this implies a total  $\gamma$ -ray energy  $\sim 10^{53} \text{ erg}$ , which is much larger than energies typically inferred in regular GRBs (Frail et al. 2001; Bloom, Frail & Kulkarni 2003). Furthermore, a comparison of the  $\gamma$ -ray energy with the remaining kinetic energy yields a ratio of  $\sim 100$ , much larger than what is typically seen in regular GRBs.

A second problem with this model arises from the observation that the relation (16) yields  $\Gamma_{\text{ini}} \Delta\theta \sim 3$  and thus,  $\Delta\theta \sim 0.1 \Gamma_{\text{ini},-1.5}^{-1}$ . This “off axis” angle is much smaller than the very wide jet opening angle  $\theta_j \sim 1$  indicated by the lack of a jet break in the X-ray afterglow observation. The probability for the ejecta being off-axis is much smaller than being on-axis. Similar considerations hold against an off-axis jet propagating into a circumburst wind.

### 4 THE THERMAL EMISSION

A soft thermal component is seen (Campana et al. 2006) in the X-ray spectrum comprising  $\sim 20\%$  of the 0.3-10 keV flux. It begins at  $\sim 152$  sec and lasts up to  $\sim 10^4$  sec. The

fitted black body temperature shows a marginal decrease ( $kT \simeq 0.16 - 0.17$  keV, with  $k$  the Boltzmann constant) and a clear increase in luminosity, by a factor of 4 in the time range 300s-2600s, corresponding to an increase in the apparent emission radius from  $R_{\text{BB,XRT}} = (5.2 \pm 0.5) \times 10^{11}$  cm to  $R_{\text{BB,XRT}} = (1.2 \pm 0.1) \times 10^{12}$  cm (Campana et al. 2006). In the sharp decline phase, the XRT emission is dominated by a thermal component ( $kT = 0.10 \pm 0.05$  keV, the corresponding apparent emission radius is  $R_{\text{BB,XRT}} = 6.6^{+14}_{-4.4} \times 10^{11}$  cm). This thermal component is undetectable in later XRT observation.

A second thermal component is detected by the UVOT. At 1.4 days  $\sim 120$  ksec the black body peak is centered within the UVOT passband. The fitted values are  $kT = 3.7^{+1.9}_{-0.9}$  eV and  $R_{\text{BB,UVOT}} = 3.29^{+0.94}_{-0.93} \times 10^{14}$  cm, implying an expansion speed of  $(2.7 \pm 0.8) \times 10^9$  cm s $^{-1}$ . This speed is typical for a supernova and it is also comparable with the line broadening observed in the optical spectra (Pian et al, 2006). The UVOT thermal component is therefore very likely dominated by the expanded hot stellar envelope (see also Campana et al. 2006).

The nature of the X-ray thermal emission is less clear. Campana et al. (2006) suggest that it arises from a shock break out from a dense wind surrounding the SN progenitor. As we have shown earlier the medium surrounding the progenitor is more likely to be constant, low density medium rather than the dense wind with a  $A_* \sim 3$  required in this model (Campana et al. 2006). We suggest, therefore, that the XRT thermal component arises from a shock heated stellar matter. As the size of the emitting black body region ( $6 \times 10^{11} - 10^{12}$  cm) is larger than the size of a typical WR- star ( $10^{11}$  cm) there are two possibilities: The emission could be from a a hot cocoon surrounding the GRB ejecta (Ramirez-ruiz, Celotti & Rees 2002; Zhang et al. 2004) and expanding initially with  $v \sim 0.1c$ . An alternative possibility is that the X-ray thermal emission arises from the shock break out from the stellar envelope. This would require, however, a progenitor's size of  $\sim 10^{12}$  cm. This is much larger than  $\sim 10^{11}$  cm or less, that is expected from a star stripped from its H, He and probably O, as inferred from the spectroscopic analysis of the SNe (Pian et al, 2006). It is not clear if stellar evolution model can accommodate such a progenitor, but surprises of this nature have happened in the past. A relativistic radiation-hydrodynamics calculations are needed to test the viability of these two possibilities. This is beyond the scope of this work.

Here we just show that a hot and optical thick outflow could account for the temporal behavior of the XRT and UVOT thermal emission. After the central engines turns off (i.e., there is no fresh hot material injected), the hot outflow expands and cools adiabatically as  $T \propto n_p^{1/3} \propto R^{-\alpha/3}$ , where  $\alpha = 3$  if the hot outflow is spreading and  $\alpha = 2$  otherwise,  $n_p$  is the number density of the particle. Once the hot region cools adiabatically so that  $kT \ll 0.2$  the thermal emission recorded by XRT in the range 0.2 to 10 keV decrease quickly with time as  $L_{\text{th,XRT}} \propto R^2 e^{-0.2\text{keV}/kT} \propto R^2 e^{-\alpha R/3R_0}$ , where  $R_0$  is the radius of the outflow at the turning off time of the central engine. The V-band flux is  $L_{\text{th,V}} \approx 4\pi\sigma R^2 T^4 \frac{y^3 \Delta y}{e^y - 1}$ , where  $y = 2.3\text{eV}/kT$ ,  $\Delta y \approx 0.13y$ , accounting for the FWHM width of V-band. For  $y \ll 1$ ,  $L_{\text{th,V}} \propto T R^2 \propto R^{2-\alpha/3} \propto t^{2-\alpha/3}$ , increases with time until

$y \sim 1$  and then it decreases rapidly. As noted by Campana et al. (2006), such a behavior is in agreement with *Swift's* observations.

## 5 DISCUSSION AND SUMMARY

The recent nearby burst GRB 060218 had many peculiar features. However, after  $\sim 10^4$  sec it had a rather usual X-ray afterglow lightcurve. Focusing on this lightcurve we draw the following conclusions.

- The non-thermal components of the afterglows can be understood within the standard fireball blast wave model, provided that the overall kinetic energy is  $5 \times 10^{50}$  erg and it has a relatively low initial Lorentz factor.
- The lack of a “jet break” up to  $10^6$  sec indicates that the outflow is wide  $\theta_j \sim 1$ .
- The medium surrounding the progenitor has a constant, low density profile rather than the expected dense stellar wind.
- The X-ray and optical/UV thermal emission cannot arise from the relativistic ejecta. A shock heated envelope of the progenitor is the most natural source. The question whether the envelope has expanded rapidly or was it initially large is open.
- While one cannot rule out that the soft spectrum and low luminosity of GRB 060218 arose due to off-axis observations we find that this is unlikely. Such a model requires a very large total energy  $\sim 10^{53}$  erg and a very large ratio of prompt  $\gamma$  energy to the remaining kinetic energy. Furthermore, this is improbable in view of the large opening angle of the relativistic ejecta  $\theta_j \sim 1$  and the small off axis viewing angle needed  $\Delta\theta \sim 0.05$ .

There are several implications to these conclusions. First we note that the wide angle of the relativistic ejecta is incompatible with the usual Collapsar model, in which a narrow jet punches a narrow hole in the envelope of a WR star (Zhang et al. 2004).

Another feature that is inconsistent with the canonical version of this model is the lack of a clear wind profile. The afterglows arises at a distance of  $R \sim 10^{17}$  cm from the central engine. It could be that the observed profile appeared arose from the interaction of the wind with the surrounding matter or it may reflect a low mass-loss rate of the progenitor star during the post-helium burning phases. A similar feature was seen also in GRB 030329. Further complications are the low initial Lorentz factor and above all the peculiar very soft and low luminosity prompt  $\gamma$  emission. This low luminosity is almost in a contrast with the fact that the total energy is comparable to the one observed in typical GRBs.

We conclude that GRB 060218 was an almost “failed GRB”. Due to some unique feature of the progenitor (a larger than usual size?) the relativistic ejecta almost did not make it across the envelope. This has lead to a wide relativistic outflow with an unusually low initial Lorentz factor. This, in turn, lead to the softer spectrum (possibly due to internal shocks taking place in a region with optical depth of order unity). A significant fraction of the energy was given to a hot cocoon and was reprocessed as a thermal emission - seen both in X-ray and later in the UV/optical. One can speculate that in many other cases the relativistic ejecta

would have stopped completely and we would have a “failed GRB”. It is possible that this is the reason why GRBs are not seen in most type Ib,c SNe (Berger et al., 2003, Soderberg et al., 2006).

## ACKNOWLEDGMENTS

We thank E. Waxman for a helpful discussion. This work is supported by US-Israel BSF and by the ISF via the Israel center for High Energy Astrophysics. TP acknowledges the support of Schwartzmann University Chair. YZF is also supported by the National Natural Science Foundation (grants 10225314 and 10233010) of China, and the National 973 Project on Fundamental Researches of China (NKBRSF G19990754). DX is at the Dark Cosmology Center funded by The Danish National Research Foundation.

## REFERENCES

Barbier L., et al., 2006, GCN 4780  
 Berger E., et al., 2003, Nature, 426, 154  
 Berger E., et al. 2003, ApJ, 599, 408  
 Bloom J. S., Frail D. A., Kulkarni S. R., 2003, ApJ, 594, 674  
 Chevalier R. A., Li Z. Y., 2000, ApJ, 536, 195  
 Campana S., et al., 2006, Nature, submitted (astro-ph/0603279)  
 Colgate S. A., 1974, ApJ, 187, 333  
 Cusumano G., et al., 2006a, GCN 4775  
 Cusumano G., et al., 2006b, GCN 4786  
 Dai Z. G., Lu T., 1998, MNRAS, 298, 87  
 De Luca A., 2006, GCN 4853  
 Fan Y. Z., Piran T., 2006, MNRAS, in press (astro-ph/0601054)  
 Frail D. A., et al., 2001, ApJ, 562, L55  
 Galama T. J., et al., 1998, Nature, 395, 670  
 Granot J., Loeb A., 2003, ApJ, 593, L81  
 Guenther E. W., 2006, GCN 4863  
 Halpern J. P., Kemp J., Piran T., Bershady M. A., 1999, ApJ, 517, L105  
 Hjorth J. et al., 2003, Nature, 423, 847  
 Huang Y. F., Cheng K. S., Gao T. T., 2006, ApJ, 637, 873  
 Lazzati D., Campana S., Ghisellini G., 1999, MNRAS, 304, L31  
 Li Z., Song L. M., 2004, ApJ, 614, L17  
 Li Z. Y., Chevalier R. A., 1999, ApJ, 526, 716  
 MacFadyen A. I., Ramirez-ruiz E. E., Zhang W. Q., 2006, Nature, submitted (astro-ph/0510192)  
 MacFadyen A. I., Woosley S. E., Heger A., 2001, ApJ, 550, 410  
 Marshall F., et al., 2006, GCN 4779  
 Mészáros P., Rees M. J., Wijers R. A. M. J., 1998, ApJ, 499, 301  
 Mirabal N., Halpern J. P., 2006, GCN 4792  
 Modjaz M., et al., 2006, ApJL, submitted (astro-ph/0603377)  
 Nousek J., et al., 2006, GCN 4805  
 O’Brien P. T., et al., 2006, ApJ, submitted (astro-ph/0601125)  
 Paczyński B., 1998, ApJ, 494, L45  
 Panaiteescu A., & Kumar P., 2001, ApJ, 560, L49  
 Pian E., et al., 2006, Nature, submitted (astro-ph/0603530)  
 Piran T., 1999, Phys. Rep., 314, 575  
 Piran T., Kumar P., Panaiteescu A., Piro L., 2001, ApJ, 560, L167  
 Piro L., et al., 1998, A&A, 331, L41  
 Ramirez-ruiz E., Celotti A., & Rees M. J., 2002, MNRAS, 337, 1349  
 Rhoads, J. E. 1999, ApJ, 525, 737  
 Sakamoto T., et al., 2006, GCN 4822  
 Sari R., Narayan R., Piran T., 1996, ApJ, 473, 204  
 Sari R., Piran T., Narayan R. 1998, ApJ, 497, L17  
 Sari R., Piran T., Halpern J. P., 1999, ApJ, 519, L17

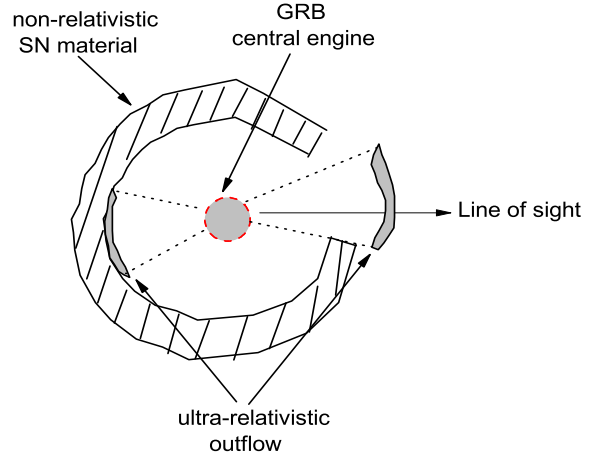


**Figure A1.** A schematic cartoon of the delayed strong thermal X-ray emission powered by the two-sided jets in supranova scenario.

Schlegel D. J., Finkbeiner D. P., Davis M., 1998, ApJ, 500, 525  
 Soderberg A., et al. 2006, ApJ, 638, 930  
 Sollerman J., et al., 2006, A&A, submitted (astro-ph/0603495)  
 Tan J. C., Matzner C. D., & McKee C. F., 2001, ApJ, 551, 946  
 Waxman E., 2004, ApJ, 605, L97  
 Waxman E., Meszaros P., 2003, ApJ, 584, 390  
 Wei D. M., Lu T., 1998, ApJ, 505, 252  
 Woosley S. E., 1993, ApJ, 405, 273  
 Woosley S. E., Zhang W. Q., Heger A., 2003, AIPC, 662, 185  
 Vietri M., Perola C., Piro, L., Stella, L., 1999, MNRAS, 308, L29  
 Vietri M., Stella L., 1998, ApJ, 507, L45  
 Vink J. S., de Koter S., 2006, A&A, in press (astro-ph/0507352)  
 Yost S., Harrison F. A., Sari R., Frail D. A., 2003, ApJ, 597, 459  
 Zeh A., Klose S., Hartmann D.H., 2004, ApJ, 609, 952  
 Zhang W. Q., Woosley S. E., Heger A., 2004, ApJ, 608, 305

## APPENDIX A: A POSSIBLE METHOD TO MEASURE THE TIME DELAY BETWEEN THE SN AND THE GRB: THE SUPRANOVA SCENARIO

The association of the GRB with the Ib/c SNe is a well established fact (e.g., Galama 1998; Hjorth 2003; Zeh et al. 2006). The time delay ( $t_{\text{delay}}$ , in units of day) between the explosion of the SN and the  $\gamma$ -ray burst is less than a few days (e.g., Hjorth et al. 2003). In the collapsar model (e.g., Woosley 1993; Paczyński 1998; MacFadyen, Woosley & Heger 2001), the explosion of the SN is simultaneous with the generation of the  $\gamma$ -ray burst. But in the supranova scenario (Vietri & Stella 1998), the SN explodes about hours to weeks earlier, depending on the dipole magnetic field of the central neutron star. So it is not very clear that which one is favored.

In the supranova model, after the collapse of the central neutron star, a black hole-disk system is formed and two sided-jets are produced (Vietri & Stella 1998; see our Fig. A1 for illustration). The  $\gamma$ -ray burst is detectable as long as the jet moving toward us has penetrated the SN material (there could be a hole left) and generated strong high energy

emission due to shocks or magnetic energy dissipation. What happens for the jet moving backward us? It has been ignored in most previous works. Li & Song (2004) assumed that this jet had emerged successfully, too and could produce a very late radio rebrightening (see also Granot & Loeb 2003). However, the chance for a relativistic jet to penetrate the SN shell is small, the reversed jet therefore is more likely to be terminated by the dense SN material and generates two shocks (see Vietri et al. 1999 for a similar discussion). One is the non-relativistic forward shock, the other is the ultra-relativistic reverse shock.

**The delayed thermal X-ray burst.** Most of the kinetic energy of the jet has been converted into the thermal energy. The forward shock energy and half reverse shock energy (i.e., the part radiating into the envelope) should be radiated thermally (see MacFadyen, Ramirez-ruiz & Zhang 2006 for similar discussion). And the typical temperature could be estimated as

$$T \approx 6 \times 10^6 \text{ K } L_{m,52}^{1/4} R_{\text{SN},14}^{-1/2}, \quad (\text{A1})$$

where  $L_m$  is the total luminosity of the outflow,  $R_{\text{SN}} \approx V_{\text{SN}} t_{\text{delay}} = 2.5 \times 10^{14} \text{ cm } V_{\text{SN},9.5} t_{\text{delay}}$  is the radius of the SN material.

The thermal emission is isotropic since the jet is non-relativistic, now. So the energy along the line of sight (reaching us through the envelope hole, see Fig. A1 for illustration) can be estimated by (see also Lazzati, Campana & Ghisellini 1999; Vietri et al. 1999)

$$E_{th} \approx \Omega_j E_m / 4\pi, \quad (\text{A2})$$

where  $\Omega_j = 2\pi(1 - \cos \theta_j)$  is the solid angle of the reverse jet,  $\theta_j$  is the half opening angle;  $E_m \approx L_m T_{90}$ , where  $T_{90} \sim$  tens seconds is the duration of the prompt high energy emission and  $L_m$  is the total luminosity of the outflow. The detected energy should be lower since part of the photons would be occulted by the central engine. The actual fraction depends on the geometry of the central engine (black hole+disk) and it is hard to estimate. As long as  $R_{\text{SN}} \sin \theta_j \gg R_{\text{disk}}$  (which seems to be the case), significant part of  $L$  should be detected, where  $R_{\text{disk}}$  is the radius of the disk.

One character of the thermal component predicted here is its delay on a timescale  $\sim 2R_{\text{SN}} \cos \theta_j / c$ , the duration should be  $\approx T_{90} + R_{\text{SN}}(1 - \cos \theta_j) / c$ . The total energy and the timescale are consistent with some soft X-ray flares detected in many GRB X-ray afterglows (e.g., Piro et al. 1998; O'Brien et al. 2006). But now the spectrum is very soft, which is inconsistent with the observation. If several hours after the GRB trigger, a strong thermal X-ray component, with a duration  $\sim$  a few hundred seconds, has been detected in the future, the supernova model is supported.

**Possible high energy emission component.** At  $R_{\text{SN}} \sim 10^{14} \text{ cm}$ , the shocked outflow itself is optical thin, the typical synchrotron radiation frequency of the reverse shock should be significant higher than that of the typical internal shocks since (i) The radius of the shock generated is about one to two order larger than that of the typical internal shocks; (ii) Currently the reverse shock Lorentz factor is  $\Gamma_{\text{sh}} \sim$  a few hundred, which is about two orders higher than that of the typical internal shocks. The minimum Lorentz factor of the shocked electrons  $\gamma_m \approx \min\{\epsilon_e[(p-2)/(p-1)](m_p/m_e)(\Gamma_{\text{sh}} - 1), \gamma_M\}$ , assuming that the shocked electrons (get  $\epsilon_e$  fraction of shock energy) take a power law

distribution  $dn/d\gamma_e \propto \gamma_e^{-p}$  for  $\gamma_m < \gamma_e < \gamma_M$ , where  $\gamma_M \sim 4 \times 10^7 B^{-1/2}$  is the maximum Lorentz factor of electron accelerated by the shock,  $B \sim 4 \times 10^8 \text{ G } \Gamma^{-1} \epsilon_{B,-2}^{1/2} L_{m,52}^{1/2} \Gamma_{\text{sh},2}$  is the magnetic field strength of the shocked region. So the typical synchrotron radiation frequency of the ultra-relativistic reverse shock is  $h\nu_{m,r} \sim 20 \text{ MeV}$  (note that now  $\Gamma \sim 1$ ). However, these photons might be absorbed by the very dense thermal background photons with energy  $\epsilon_a \sim 2(m_e c^2)^2 / h\nu_{m,r} \sim 25 \text{ keV}$ , and generate relativistic  $e^\pm$  pairs with random Lorentz factor  $\gamma_{\text{pair}} \sim 20$ . Here we estimate its typical pair-production radius  $R_{\text{pair}} \sim 1/(n_{\epsilon_a} \sigma_T)$ , where  $n_{\epsilon_a} \sim [\pi^2(\hbar c)^3]^{-1}(\Omega_j/4\pi)\epsilon_a^3 / [\exp(\epsilon_a/kT) - 1]$  is the number density of the thermal photons with energy  $\epsilon > \epsilon_a$ . For the typical values taken here,  $R \sim 10^{12} \text{ cm} \gg cT_{90}/4\Gamma_{\text{sh}}$ . Therefore most pairs are generated outside of the shocked material and would not change the reverse shock emission. These relativistic pairs will lose their energy mainly through inverse Compton scattering with the thermal photons and boost them to the  $\sim \gamma_{\text{pair}}^2 kT \sim$  a few hundred keV energy range. This component might be detectable, too. The lack of the detection of a  $\gamma$ -ray re-burst in GRB 030329 may support the collapsar model.